Resonance production in relativistic heavy ion collisions in a binary emission model

Subrata Pal

Department of Nuclear and Atomic Physics, Tata Institute of Fundamental Research, Homi Bhabha Road, Mumbai 400005, India
(Received 17 April 2008; revised manuscript received 20 June 2008; published 28 July 2008)

Resonance particle ratios and spectra are calculated in the sequential binary emission model for hadrons produced from the decay of a single massive resonance formed in relativistic heavy ion collisions. The sequential model which is quite successful in reproducing the yield ratios for stable hadrons at energies currently available at the BNL Relativistic Heavy Ion Collider (RHIC) is found to describe remarkably well the yield ratios for the resonances $K^*(892)^0$ and ϕ mesons. The model indicates a short expansion time between the average chemical and thermal freeze-out with negligible regeneration of the resonances via the inverse two-body elastic collision process. Model estimates of the yield ratios for the strange baryons $\Lambda(1520)$ and $\Sigma(1385)$ are presented.

A major goal of research in relativistic heavy ion collisions is to study the properties of hot and dense matter and the possible transition from hadronic matter to a deconfined quark-gluon plasma. The hadronic resonances that may be produced at different stages of collisions, depending on their lifetimes, can provide useful information on the dynamics and evolution of matter produced in these collisions. In particular, resonance multiplicities and spectra and their yield ratios with stable hadrons are the most interesting probes of the nature, composition, and size of the medium in which they are produced.

The extent of rescattering of the resonance decay products in a medium lead to the concept of chemical freeze-out (inelastic processes cease) and subsequent kinetic freeze-out (elastic process ceases and the system decouples). In contrast to the expected scenario of chemical freeze-out followed by thermal freeze-out (at the temperature $T_{\rm th} \simeq 120$ MeV) [1], the simultaneous chemical and thermal freeze-out of hadron gas was also shown [2] to describe particle yield ratios and spectra at the BNL Relativistic Heavy Ion Collider (RHIC).

We have developed a model [3] for particle production via sequential binary emission of heavy resonances (Hagedorn states), low-lying measured light resonances and stable hadrons. The model is in good agreement with the CERN Super Proton Synchrotron (SPS) and RHIC heavy ion collision data for the *stable* hadron yield ratios and their spectra with a mass spectra (Hagedorn) temperature of $T_H \approx 170$ MeV and an average transverse flow velocity of $\langle \beta_t \rangle = 0.27c$. The Hagedorn temperature deduced from best fit of the data is similar to the critical temperature of $T_{\rm cr} \approx 170$ MeV for a QGP phase transition in the lattice QCD simulations at vanishing baryon density [4], and it is also close to the chemical freeze-out temperature extracted from fits to the RHIC data in the statistical hadron gas model [5].

To gain insight into the dynamical evolution of matter produced at RHIC, we investigate in this Rapid Communication the resonance production within the sequential binary emission model and compare the abundances with the RHIC data. We focus mainly on two meson resonances, a short-lived $K^*(892)^0$ and a relatively long-lived $\phi(1020)$, as well as the baryon resonances $\Lambda(1520)$ and $\Sigma(1385)$.

In the sequential binary emission model employed here, we assume that a massive resonance fireball is formed in

the overlapping region of the colliding nuclei. The resonance subsequently decays by the emission of two particles that may be resonance(s) and/or stable hadron(s). The binary decay chain continues till all stable particles are formed. Depending on whether each of the daughter masses are below or above an adopted threshold continuum mass of $m_{\rm th}^c = 2$ GeV, a binary decay is characterized by three outgoing channels: (i) both daughters are low-lying measured *discrete* resonances and/or stable hadrons, (ii) one daughter is a massive resonance in the continuum (Hagedorn state) and the other a discrete particle, and (iii) both daughters are in the continuum. A brief outline is presented here, the details can be found in Ref. [3].

Experimental information on the Hagedorn states that increase sharply with the mass of a hadron is unknown. Based on the Hagedorn hypothesis [6], we have assumed that the mass spectra grow nearly exponentially [3,7]:

$$\rho(m, q) = A \frac{\exp[\{m - m_g f(m - m_g)\}/T_H]}{[\{m - m_g f(m - m_g)\}^2 + m_r^2]^\alpha}. \quad (1)$$

For a mass m characterized by its quantum number $q \equiv (B, S, J, I, I_z)$, its ground-state mass is parametrized by

$$m_g(q) = a_Q(\max|3B + S|, 2I) + a_S|S|. \quad (2)$$

The parameters $a_Q = 0.387$ and $a_S = 0.459$ GeV are obtained from fits to all the measured *smallest* masses. The factor $f(m - m_g)$ suppresses the effect of m_g at high m, and it is approximated as

$$f(m - m_g) \simeq \frac{1}{1 + [(m - m_g)/m_f]^n}, \quad (3)$$

where we have set the exponent $n = 1$ and $m_f = 2$ GeV. At a given T_H, the exponent α in Eq. (1) is evaluated by comparing the theoretical and experimental cumulants of the spectrum [3, 7]. For small masses $m < m_{\rm th}^c$, we employed all the measured stable hadrons and resonances given in the *Particle Data Book*.

The resonance formation cross section in a two-body collision, $q_1 + q_2 \to q$, is given by [3]

$$\sigma(q_1 + q_2 \to q) = \frac{2\pi m_1 m_2}{m p^\star} \rho(m, q) |\mathcal{M}_{q_1+q_2 \to q}|^2, \quad (4)$$

where p^* is the c.m. momentum. In Eq. (4), and hereafter, the spin degeneracy $(2J + 1)$, originating from initial and final

state spin averaging of matrix element square $|\mathcal{M}_{q_1+q_2 \to q}|^2$, has been absorbed into the continuum density of states ρ. The simple geometric fusion cross section can be written as

$$\sigma(q_1 + q_2 \to q) = \mathcal{C}_I \pi R^2, \qquad (5)$$

where $\mathcal{C}_I = \langle I_1 I_{z_1} I_2 I_{z_2} || I I_z \rangle$ represents the Clebsch-Gordan coefficients for the isospins, and R the radius of the fused resonance of mass m. Equations (4) and (5) allow us to extract $|\mathcal{M}_{q_1+q_2 \to q}|^2$, which is to be used in the calculation of the decay widths.

The general expression for the decay width into a binary channel $q \to q_1 + q_2$ is obtained by integrating the density of states over the available phase space

$$
\begin{aligned}
&\Gamma(q \to q_1 + q_2) \\
&= \int \frac{d\mathbf{p}}{(2\pi)^3} \int dm'_1 \frac{m'_1 \rho(m'_1, q_1)}{e_1(\mathbf{p})} \int dm'_2 \frac{m'_2 \rho(m'_2, q_2)}{e_2(\mathbf{p})} \\
&\quad \times |\mathcal{M}_{q \to q_1+q_2}|^2 \, 2\pi \, \delta\left(e_1(\mathbf{p}) + e_2(\mathbf{p}) - m\right).
\end{aligned} \qquad (6)
$$

For case (i) with both daughters as discrete particles, the state densities are $\rho_j(m'_j) = (2J_j + 1)\delta(m'_j - m_j)$. Using detailed balance $|\mathcal{M}_{q \to q_1+q_2}|^2 = |\mathcal{M}_{q_1+q_2 \to q}|^2$, the decay width of Eq. (6) then reduces to

$$\Gamma^{(i)}(q \to q_1 + q_2) = \mathcal{C}_I \frac{(2J_1 + 1)(2J_2 + 1)p^{\star 2}(m_1, m_2)R^2}{2\pi\rho(m, q)}. \qquad (7)$$

For the decay channel (ii), assuming q_1 to be the discrete particle, $\ln \rho_2$ for the continuum daughter resonance is expanded about the lower limit $\mathbf{p} = 0$, to give the approximate decay width [3]

$$
\begin{aligned}
&\Gamma^{(ii)}(q \to q_1 + q_2) \\
&= \mathcal{C}_I \frac{(2J_1 + 1)m R^2 T_2^2(T_2 + m_1)}{\pi m_2} \frac{\rho(m_2, q_2)}{\rho(m, q)}, \quad (8)
\end{aligned}
$$

where the mass of the continuum daughter particle is $m_2 = m - m_1$ and the effective emission temperature is $T_2 = -[\partial \ln \rho_2 / \partial e_1(p)]_{e_1=m_1} \approx m/(m_2 T_H)$.

For the decay channel (iii), we have used a simplified nonrelativistic expansion as both masses are in the continuum [3].

During dynamical evolution, binary collisions between hadrons in the hadron resonance gas model may regenerate the resonance thereby maintaining a detailed balance [3]. Based on a relativistic transport (ART) model [8] (see also Ref. [9]), dominant elastic and inelastic $2 \leftrightarrow 2$ collision channels with explicit isospin degrees of freedom have been included. For baryon-baryon scatterings, we have included resonance production via $(N\Delta N^*)(N\Delta N^*) \leftrightarrow (N\Delta N^*)(N\Delta N^*)$; the cross sections and other details can be found in Ref. [8]. For meson-baryon scatterings, the direct (elastic) reactions $(\pi\rho)(N\Delta N^*) \leftrightarrow (\pi\rho)(N\Delta N^*)$ and inelastic (anti)kaon production channels $(\pi\rho\omega\eta)(N\Delta N^*) \leftrightarrow K(\Lambda\Sigma)$ and $\pi(\Lambda\Sigma) \leftrightarrow \bar{K}(N\Delta N^*)$ are included. Kaon-baryon elastic scatterings are included with a constant cross section of $\sigma_{el}(KB) = 10$ mb [8]. Meson-antibaryon collisions have been accordingly taken into account. For meson-meson collisions, apart from $\pi\pi \leftrightarrow \rho\rho$, $\pi\eta$, $\eta\eta$ reactions, kaon production from inelastic
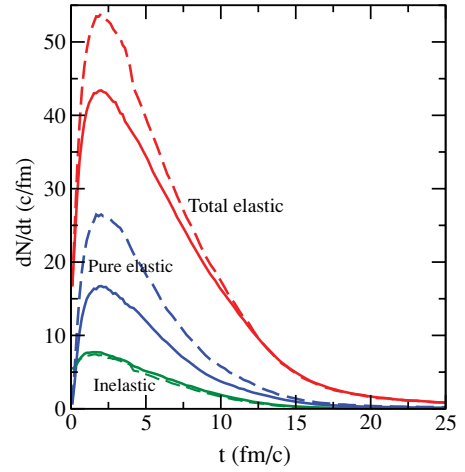

FIG. 1. (Color online) Collision rates in the binary emission model at $T_H = 170$ MeV from an initial fireball of mass $m_0 = 100$ GeV, baryon number $B_0 = 3$, and strangeness $S_0 = 0$ for elastic scattering cross section of $\sigma_{el} = 5$ mb (solid lines) and $\sigma_{el} = \sigma_{el}(KB) = 20$ mb (dashed lines); see text for details.

scattering $(\pi\eta)(\pi\eta) \leftrightarrow K\bar{K}$ and $(\rho\omega)(\rho\omega) \leftrightarrow K\bar{K}$, and K^* production via $(\pi\eta)(\rho\omega) \leftrightarrow K^*\bar{K}, \bar{K}^*K$ are included. For all other elastic collisions, a constant cross section of $\sigma_{el} = 5$ mb is used.

Calculations are performed in a Monte Carlo fashion starting with a fixed initial value of a single resonance of $m_0 = 100$ GeV, $B_0 = 3$, and $S_0 = 0$ (strangeness neutral), and a Hagedorn temperature of $T_H = 170$ MeV that best describes the data for stable hadron yield ratios in central Au+Au collisions at $\sqrt{s} = 130A$ GeV at RHIC [3].

Shown in Fig. 1 are the time evolution of the inelastic and elastic collision rates (solid lines) in this model. The inelastic collision rate is defined as a flavor-changing process (strangeness production/absorption) in the resonance decay/formation and in inelastic $2 \leftrightarrow 2$ collisions. The elastic collision rate comprises two components: the flavor-nonchanging particle resonance formation/decay and a pure $2 \leftrightarrow 2$ elastic scattering.

At the early stage of the evolution, the decay channel (ii) dominates with the emission of a light particle and a residual heavy resonance. The large masses of the decaying resonances at this stage make the decay widths considerably large. As the particle density is high, recombination and the $2 \leftrightarrow 2$ process are also rapid, resulting in a strong increase in the inelastic and elastic collision rates. The strangeness-changing (inelastic) channel increases the ground-state mass m_g of the residual nucleus, resulting in a smaller branching ratio than in the strangeness-fixed (elastic) process. Consequently, at all times, the elastic collision rate dominates the inelastic flavor-changing process. Even after $t \simeq 15$ fm/c when the inelastic process has died down (chemical freeze-out), the system still undergoes elastic collision where the momentum of hadrons are likely to change while their abundances remain practically unaltered (kinetic freeze-out). At all times, the flavor-nonproducing elastic rates are somewhat larger than the pure $2 \leftrightarrow 2$ elastic collision rates.

We now employ the combined measurements of the resonances ϕ and $K^*(892)^0$ to gain insight into the breakup dynamics of the source. A direct confrontation of the abundance ratios in this model with the experimental data [10,11] should verify the proposed scenario. The daughter particles from decay of the resonances may suffer rescattering in the matter and thus cannot be reconstructed.

The total number of $K\bar{K}$ pairs formed from ϕ meson decay up to an average 'freeze-out' time of $t_f = 40$ fm/c, considered in the calculation, is given by [9]

$$N_{K\bar{K}} = \int_0^{t_f} dt\, N_\phi(t)\Gamma_{\phi \to K\bar{K}} + N_\phi(t_f)\frac{\Gamma_{\phi \to K\bar{K}}}{\Gamma_\phi}, \qquad (9)$$

where $N_\phi(t)$ denotes the number of ϕ mesons at time t. The final ϕ meson abundance is obtained by dividing the above expression by the $K\bar{K}$ branching ratio $\Gamma_{\phi \to K\bar{K}}/\Gamma_\phi$. The same procedure is used to calculate the abundances for K^{*0} mesons from πK decay and the baryon resonances $\Lambda(1520)$ and $\Sigma(1385)$ from the respective decay channels $\Lambda(1520) \to \bar{K}N$ and $\Sigma(1325) \to \pi\Lambda$.

Figure 2 (top panel) shows the time evolution of ϕ meson abundance (solid line) in this model. The ϕ meson with a small decay width has a larger probability of decaying outside the system and can be detected. At times $t \lesssim 15$ fm/c, the ϕ production and decay are mainly from the heavy resonance states, where the production rate dominates over its annihilation from an inverse two-body collision. In contrast, during this stage the contribution from decay and formation rates via the channel $\phi \leftrightarrow K\bar{K}$, though identical, are very small. At a later time, the surviving ϕ mesons decay outside the fireball to $K\bar{K}$ pairs even though there is considerable late ϕ meson production from the inverse process.

To facilitate comparison with the STAR data at RHIC [11], the K^{*0} in this paper refers to the average of K^{*0} and $\bar{K}^{*0}$. For the K^{*0} meson with a lifetime ($\Delta t \approx 4$ fm/c) comparable to the source, its decay products suffer strong rescattering and are less likely to be reconstructed (resulting in a small K^{*0}/K ratio). The overall net effect of rescattering and regeneration via $\pi K \to K^{*0}$ on the total yield depends on the expansion time between chemical and thermal freeze-out and the magnitude of the interaction cross sections of π and K. Figure 2 (bottom panel) displays the time evolution of K^{*0} meson in the model. In contrast to ϕ, the K^{*0} abundance peaks at an earlier time of $t = 8$ fm/c and rapidly decays thereafter. As for ϕ meson, the production overwhelms the annihilation rate of K^{*0} at $t \lesssim 8$ fm/c primarily due to decay and formation of Hagedorn states, respectively. The rates for K^{*0} are larger than for ϕ because of the former's smaller mass and larger width. At a later time, the decay of $K^{*0} \to \pi K$ becomes the most effective channel; the regeneration of K^{*0} from the inverse channel is relatively smaller at this expanding stage.

Collective transverse flow effects are incorporated into this model by considering a uniform transverse velocity distribution $d^2N/d\beta_t^2 = \Theta(\beta_t - \beta_{max})$ [3]. The transverse mass spectra of stable (non)strange particles and antiparticles are well reproduced for central Au+Au collisions at the RHIC energy of $\sqrt{s} = 130A$ GeV with one common average transverse velocity of $\langle\beta_t\rangle = 2\beta_{max}/3 \approx 0.27c$. In Fig. 3, we show the boosted transverse mass spectra with the same boost velocity $\langle\beta_t\rangle = 0.27$ for ϕ and K^{*0} mesons for all the produced resonances (dashed line) and that reconstructed from unscattered (solid line) decay pairs $K\bar{K}$ and πK, respectively. It is seen that the particle abundances are suppressed primarily at low m_T due to the rescattering of the decay products; this
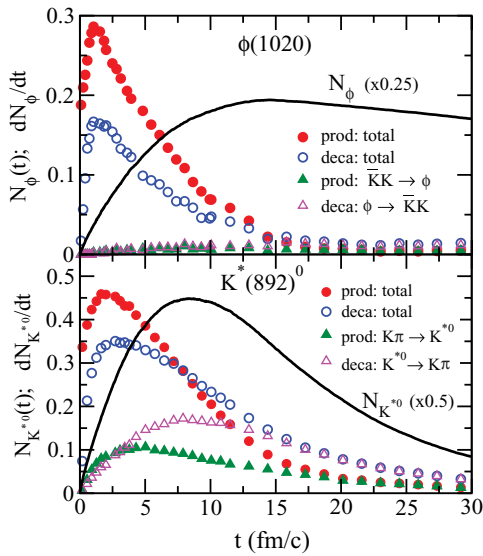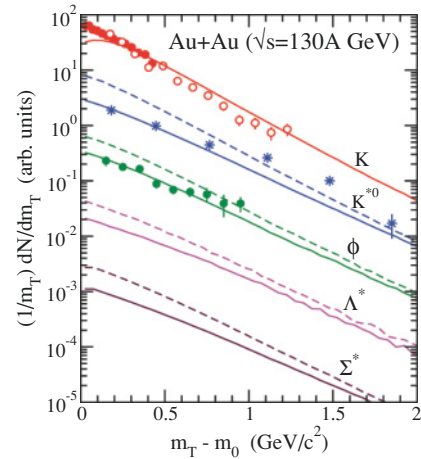

FIG. 2. (Color online) Time evolution of abundances, production, and decay rates for ϕ meson (top panel) and K^{*0} (bottom panel) in the decay model with the same input parameters of Fig. 1 and $\sigma_{el} = 5$ mb. The abundances are shown in thick solid lines. The circles refer to the total production and decay rates, and the triangles correspond to rates for $\phi \leftrightarrow K\bar{K}$ (top panel) and $K^{*0} \leftrightarrow \pi K$ (bottom panel).

FIG. 3. (Color online) Transverse mass spectra for the K, K^{*0}, ϕ, Λ^*, and Σ^* in the binary emission model with input parameters of Fig. 1 and $\sigma_{el} = 5$ mb. The results are for all (dashed lines) resonances produced in the system and for the corresponding reconstructed ones (solid lines) whose daughter pairs have not scattered at all. The symbols are the data for central Au+Au collision at $\sqrt{s} = 130A$ GeV from the STAR Collaboration for K (solid squares) [12], K^{*0} [11], and ϕ [10], and from the PHENIX Collaboration for K (open squares) [13].

feature is also prevalent without the boost. Since the transverse momentum of a particle increases with increasing scattering and because of the pressure buildup in the system, the decayed particles at an early stage, which are predominantly scattered, have low m_T. As the decay products of K^{*0} are mostly rescattered, it exhibits a larger suppression than ϕ. This suppression leads to a higher apparent slope temperature T for the reconstructed resonances. For K^{*0} this is estimated to be $T_{K^{*0}} = 320$ MeV at $0.1 < p_T < 2$ GeV/c, which is somewhat smaller than that in the STAR data at RHIC [11].

The transverse mass spectra for the baryons $\Lambda(1520)$ and $\Sigma(1385)$ identified from their decay products $\Lambda(1520) \rightarrow \bar{K}N$ and $\Sigma(1385) \rightarrow \pi\Lambda$ are also shown in Fig. 3. To increase the statistics, we have summed $\Sigma^* = \Sigma^{\pm,0}(1385)$. The ratios $\bar{\Lambda}^*/\Lambda^* \approx \bar{\Sigma}^*/\Sigma^* \approx 0.75$ have been found. The rescattering of the decay products leads to large collective flow for the reconstructed Λ^* and especially Σ^*, which is further aided by their large masses.

Summed over all rapidities, the ratio of the abundances of a resonance reconstructed from decay pairs that have not suffered any collision to all the resonance produced in the system is $N_{R/A} = 0.79, 0.47, 0.53$, and 0.47 for ϕ, K^{*0}, Λ^* and Σ^*, respectively. Though the lifetime of Σ^*, $\tau_{\Sigma^*} = 5.5$ fm/c, is longer than that of K^{*0}, their identical $N_{R/A} = 0.47$ stems from heavier and thereby slowly moving Σ^* whose decay products suffer appreciable scattering.

In Table I, the RHIC data for the yield ratios are compared with the corresponding ratios in the binary emission model for total abundances and for the reconstructed resonances; here K is the average of K^+ and K^-. Feed-down contributions from heavier particles are included for the stable hadrons. The ratio ϕ/K^{*0}, which measures strangeness suppression, increases by reconstruction because of the enhanced suppression of K^{*0} compared to that of ϕ meson. The overall good agreement obtained in our model between the reconstructed ratios and the data could indicate that the continuum Hagedorn states provide an alternative scenario to quark-gluon plasma proposed [14] to explain strangeness enhancement at RHIC and SPS. The suppressed K^{*0}/K, Λ^*/Λ, and Σ^*/Λ ratios suggest that

rescattering dominates regeneration in the medium between chemical and kinetic freeze-out.

In conjunction with the excellent model agreement of the yield ratios to the RHIC data, the resonance spectra also exhibit features that are qualitatively similar to the data [10,11]. From Fig. 3, it is evident that though the slope temperature of reconstructed K^{*0} is larger than that of kaons due to higher mass and thereby larger flow, the slope temperatures follow $T_{K^{*0}} = T_\phi$ and $T_{\Lambda^*} = T_{\Sigma^*} = 360$ MeV. The present decay model thus suggests a scenario of sudden expansion of the system, i.e., a short duration between the average chemical and thermal freeze-out. This is evident from Figs. 1 and 2 where the scattering/production rates peak at $t = 3$–5 fm/c and drop exponentially thereafter with little regeneration. The fact that the measured ratios for K^{*0} are also well reproduced in the thermal model [5] at chemical freeze-out suggests a scenario of short expansion time between the average chemical and thermal freeze-out.

The yield ratios have been also calculated for the $158A$ GeV Pb+Pb central collisions at the SPS energy and for $14.6A$ GeV/c Si+Au(Pb) central collisions at the BNL Alternating Gradient Synchrotron (AGS). Fairly good reproduction for stable hadron ratios at the SPS energy can be obtained with an initial baryon number to mass ratio of $B_0/m_0 = 0.25$ GeV^{-1} at a $T_H = 170$ MeV [3]. The hadron yield ratios of Refs. [15] at the AGS can be reproduced with a larger net baryon content of $B_0/m_0 = 0.54$ GeV^{-1} at $T_H = 170$ MeV and a weaker insensitivity on the minimum mass m_g in the mass spectra of Eq. (1). The latter is achieved by increasing the factor $f(m - m_g)$ in Eq. (3) by reducing n to 0.5 from the 'standard' value of $n = 1$. The results at the higher SPS and RHIC energies are rather unaffected by such changes.

In Fig. 4, we show the energy dependence of various ratios calculated for reconstructed resonance yields. With increasing energy of collision, K^{*0}/h^- and ϕ/h^- exhibit strong increases

TABLE I. Particle ratios calculated in the decay model at mass spectrum temperature of $T_H = 170$ MeV with initial baryon to mass ratio of $B_0/m_0 = 0.03$ GeV^{-1} compared to the RHIC data for central Au+Au collisions at $\sqrt{s} = 130A$ GeV [10,11]. Model calculations are for all resonances produced in the system and those reconstructed from the decay products that have not suffered any collision with $\sigma_{el} = 5$ mb.

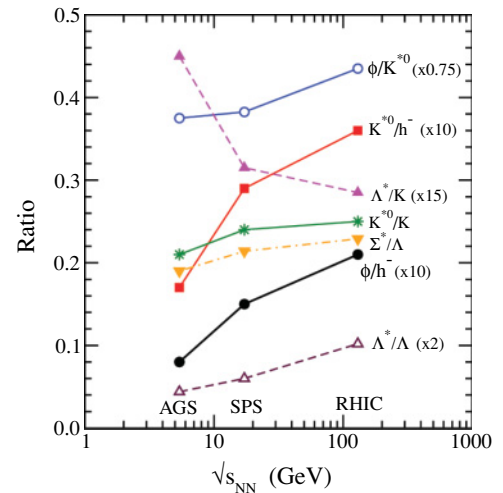| Ratio	All	Reconst.	Data
$\bar{K}^{*0}/K^{*0}$	0.93	0.93	0.92 ± 0.14
K^{*0}/h^-	0.078	0.036	$0.042 \pm 0.004 \pm 0.01$
K^{*0}/K	0.55	0.25	$0.26 \pm 0.03 \pm 0.07$
ϕ/h^-	0.027	0.021	0.021 ± 0.001
ϕ/K^{*0}	0.34	0.58	$0.49 \pm 0.05 \pm 0.12$
Λ^*/K	0.035	0.019	
Λ^*/Λ	0.095	0.051	
Σ^*/Λ	0.49	0.23	

FIG. 4. (Color online) Energy dependence of the reconstructed yield ratios in binary emission model with input parameters adjusted separately to reproduce the overall stable hadron yield ratios for central heavy ion collisions at AGS, SPS, and RHIC energies.

indicating that K^{*0} and ϕ abundances increase faster than negatively charged hadrons. The ratios K^{*0}/K and Σ^*/Λ are seen to be less sensitive to $\sqrt{s_{NN}}$. As the net baryon content of the system decreases with increasing energy, Λ^*/K is seen to decrease and thus $\bar{\Lambda}^*/K$ increases (not shown).

Calculations at the RHIC energy are repeated with a larger elastic scattering cross section $\sigma_{\rm el} = \sigma_{\rm el}(KB) = 20$ mb in contrast to the $\sigma_{\rm el}(KB) = 10$ mb and $\sigma_{\rm el} = 5$ mb used above. As evident in Fig. 1, the pure and thereby the total elastic rates (dashed lines) are enhanced. The ratio of the reconstructed to the total yield for the resonances ϕ, K^{*0}, Λ^*, and Σ^* are $N_{R/A} = 0.78, 0.42, 0.52,$ and 0.44, respectively. The particle abundance ratios (all, reconstructed) turn out to be $K^{*0}/h^- = (0.076, 0.032)$, $K^{*0}/K = (0.54, 0.23)$ and $\phi/K^{*0} = (0.34, 0.65)$ for mesons, and $\Lambda^*/K = (0.032, 0.017)$, $\Lambda^*/\Lambda = (0.088, 0.047)$, and $\Sigma^*/\Lambda = (0.47, 0.21)$ for baryons. The enhanced rescattering of the decay products leads to somewhat smaller yield ratios of the reconstructed resonances to stable hadrons as compared to those in Table I with $\sigma_{\rm el} = 5$ mb.

In summary, we have studied the production of resonances in relativistic heavy ion collisions within the sequential binary emission model. The reconstructed yield ratios involving the resonances K^{*0} and ϕ mesons agree remarkably well with RHIC data for the same set of parameters used to reproduce the stable hadron yield ratios at this energy [3]. From the nearly identical transverse mass spectra for the mesons and baryons and from the collision rate, it seems that the present model supports a scenario of a rather short expansion time between the average chemical and thermal freeze-out with negligible regeneration of the resonances from the decay products.

---

[1] M. Bleicher and J. Aichelin, Phys. Lett. **B530**, 81 (2002).

[2] W. Broniowski and W. Florkowski, Phys. Rev. C **65**, 064905 (2002).

[3] S. Pal and P. Danielewicz, Phys. Lett. **B627**, 55 (2005).

[4] F. Karsch, E. Laermann, and A. Peikert, Nucl. Phys. **B605**, 579 (2001); F. Karsch and E. Laermann, arXiv:hep-lat/0305025.

[5] A. Andronic, P. Braun-Munzinger, and J. Stachel, Nucl. Phys. **A772**, 167 (2006).

[6] R. Hagedorn, Suppl. Nuovo Cimento **3**, 147 (1965).

[7] W. Broniowski and W. Florkowski, Phys. Lett. **B490**, 223 (2000).

[8] B.-A. Li and C. M. Ko, Phys. Rev. C **52**, 2037 (1995).

[9] Z. W. Lin, C. M. Ko, B.-A. Li, B. Zhang, and S. Pal, Phys. Rev. C **72**, 064901 (2005).

[10] C. Adler *et al.* (STAR Collaboration), Phys. Rev. C **65**, 041901 (2002).

[11] C. Adler *et al.* (STAR Collaboration), Phys. Rev. C **66**, 061901 (2002).

[12] C. Adler *et al.* (STAR Collaboration), Phys. Lett. **B595**, 143 (2004).

[13] K. Adcox *et al.* (PHENIX Collaboration), Phys. Rev. Lett. **88**, 242301 (2002).

[14] P. Koch, B. Müller, and J. Rafelski, Phys. Rep. **142**, 67 (1986).

[15] T. Abbott *et al.* (E802 Collaboration), Phys. Rev. C **50**, 1024 (1994); G. S. F. Stephans *et al.* (E802 Collaboration), Nucl. Phys. **A566**, 269c (1994); S. E. Eiseman *et al.* (E810 Collaboration), Phys. Lett. **B325**, 322 (1994).